Available online at www.sciencedirect.com
SciVerse ScienceDirect
Energy Procedia 37 (2013) 5929 – 5937
Energy Procedia

GHGT-11

Carbonation of activated serpentine for direct flue gas mineralization

Mischa Werner[a], Subrahmaniam B. Hariharan[a], Andressa V. Bortolan[a], Daniela Zingaretti[b], Renato Baciocchi[b], Marco Mazzotti[a]*

[a]*Institute of Process Engineering, ETH Swiss Federal Institute of Technology, Sonneggstrasse 3, CH-8092 Zurich, Switzerland*
[b]*Department of Civil Eng. and Computer Science Eng., University of Rome "Tor Vergata", Via del politecnico 1, 00133 Rome, Italy*

Abstract

Research in mineral carbonation has moved towards process concepts that combine the capture of CO_2 from flue gas with its conversion into stable carbonates. This requires highly reactive source materials that dissolve under lean CO_2 pressures and temperatures. Activated serpentine has been used in this study, and its carbonation potential under flue gas conditions has been investigated. Single-step carbonation experiments were performed in stirred reactors with gas-dip tubes, at partial pressures of CO_2 up to 1 bar, temperatures between 30°C and 90°C, with and without concurrent grinding using a ball mill. The pH and solids were monitored in-situ, and the degree of carbonation of the products was quantified using thermogravimetric analysis. Given the low CO_2 pressure, carbonation was successful, as confirmed by the formation of the two magnesium carbonates nesquehonite and hydromagnesite. However, under all conditions investigated, including grinding, the extent of carbonation did not exceed 20%. It was concluded that after the onset of precipitation, the reactor solution in single-step carbonation experiments reaches equilibrium conditions with respect to both serpentine dissolution and carbonate precipitation.

Selection and/or peer-review under responsibility of GHGT

Keywords: Flue gas mineralization; Single-step carbonation; Activated serpentine; Magensium carbonate; TGA analysis

1. Introduction

Global emissions of CO_2 keep rising fast while the deployment of conventional CCS technologies is slow. For experts, storing CO_2 underground serves the purpose of greenhouse gas emission mitigation. However, such benefit is not necessarily recognized by the general public. Instead, the fear of leakage and of depreciation of private property dominates the perception of the technology. Consequently, alternatives

* Corresponding author. Tel.: +41-44-632-2456; fax: +41-44-632-1411.
E-mail address: marco.mazzotti@ipe.mavt.ethz.ch

1876-6102
Selection and/or peer-review under responsibility of GHGT
doi:10.1016/j.egypro.2013.06.519

to subsurface storage, such as mineral carbonation or utilization concepts, have started to draw both industry's and policymaker's attention. Mineral carbonation involves the following reactions: 1) CO_2 dissolution into an aqueous phase, 2) leaching of magnesium/calcium from natural minerals or industrial residues, 3) precipitation of Mg-/Ca-carbonates. This sequence leaves room for several process options, from single-step carbonation, where all three reactions take place in the same batch, to multi-step strategies, where process conditions can be tuned to promote each reaction separately. The slow kinetics of reaction 2 makes energy intensive mechanical and/or thermal feedstock activation inevitable. While this adds up on costs, the benefit of an immediate storage in solid form without risking public opposition is obvious but difficult to monetize. If the CO_2 stream were to be concentrated in a preceding capture step, overall costs would exceed those for conventional CCS by far. Hence, the focus in mineral carbonation R&D has moved towards process concepts that combine the capture of CO_2 from an industrial off-gas with its simultaneous conversion into stable carbonates. Capture is promoted by the dissolving feedstock, which provides alkalinity to the solution, enabling the latter to take up more CO_2. However, to dissolve under low partial pressures of CO_2, the feedstock material must be highly reactive. Direct flue gas mineralization might only be successful if started from scarce feedstock materials such as special industrial wastes, or by means of pH-tuning additives that are difficult to recover. An alternative is offered by the activation of the mineral serpentine [1]. Natural serpentine outplays other sources of alkaline earth metals regarding occurrence and abundance, and it can be heat-treated to maximize reactivity. Thermal activation above 600°C removes enough chemically bound water to destabilize the crystal lattice into a pseudo amorphous structure. In early studies, where traditionally pre-captured CO_2 was used, such heat activation was concluded to be economically unfeasible [2, 3].

In our lab, with serpentine that was ground into particle sizes below 125 μm and thermally activated at 610°C, we measured dissolution to be 2-3 orders of magnitude faster than for olivine, even in the absence of additives. Building up on this promising result, the focus of the present study was set to the precipitation of Mg-carbonates in the serpentine-CO_2-H_2O system. The goal was to explore the carbonation potential of activated serpentine in its most simple process option, the single step carbonation.

2. Background

Typical flue gas CO_2 concentrations range from 4% for gas fired power plants up to over 20% for cement plants. Elevated partial pressures of CO_2, p_{CO2}, would require the co-compression of the other off gases, which is far from energetically efficient. Hence, the operating p_{CO2} for a flue gas mineralization process must not exceed levels close to ambient pressure or below. As to temperature, operating conditions are also limited to moderate levels, owing to the decreased solubility of CO_2 in water with increasing temperature. From a thermodynamic point of view, the anhydrous form magnesite ($MgCO_3$) is the only stable Mg-carbonate in the system MgO-CO_2-H_2O at all temperatures and p_{CO2} [4]. Hänchen et al. [5] calculated the solubilities of different magnesium carbonates using the geochemical equilibrium software EQ3/6 [6] and a database therein that employs a Debey-Hückel model for the activity coefficients (see Fig. 1).

However, kinetics rather than thermodynamics govern the precipitation regime of the Mg-carbonate system. In fact, numerous studies reported nesquehonite ($MgCO_3.3H_2O$) to be the first precipitate to form under lean p_{CO2} conditions and low temperatures [5 and references therein]. The formation of the basic carbonate hydromagnesite ($(MgCO_3)_4.Mg(OH)_2.4H_2O$) is favored at higher temperatures and high pH values. At a pH lower than 9, nesquehonite can form up to temperatures above 60°C [7]. If nesquehonite is exposed to temperatures higher than 50°C, it transforms into hydromagnesite over time [e.g. 8].

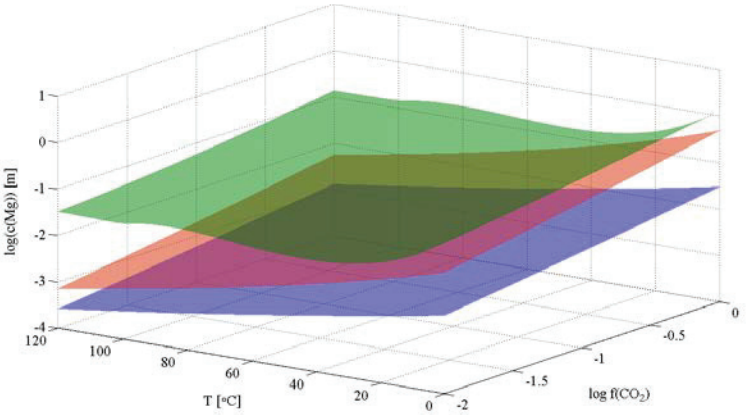

Fig. 1. Solubilities of magnesite (blue), hydromagnesite (red), and nesquehonite (green) at flue gas mineralization conditions [5].

3. Methods

3.1. Experimental

Activated serpentine was received from Shell Global Solutions Int, Amsterdam, the Netherlands. The original serpentine ($(Mg,Fe,Ca,\ldots)_3Si_2O_5(OH)_4$) has been ground to a particle sizes below 125 µm and heat treated at 610°C by the provider, thus removing 75% of the hydroxyl groups. Upon acid digestion, the composition of the activated serpentine has been measured by the authors using ICP-OES (Agilent, 710-ES), which indicated a magnesium content of 20.35% by weight. Slurries have been prepared using ultrapure water. Nitrogen (grade 5, 99.999% pure), CO_2 (grade 3, 99.9% pure), and a mixture of the two (±2% relative tolerance) were bought from Pangas, Switzerland. Two 100 ml galss reactors in an Easymax^{TM} synthesis workstation for chemical and process development (Mettler Toledo, Switzerland) have been equipped with gas dip tubes and rotameters to control the flow of the process gas. The reactor lids hosts ports for reflux-condensers, as well as for a pH- and Raman-probe to monitor dissolving and precipitating species in-situ.

Upon filling the reactors with the designated amount of water, first nitrogen and then CO_2 (or the mixture) have been bubbled through the solution for 30 min each, to remove oxygen and to establish the initial conditions with respect to temperature and p_{CO2}. The start of an experiment corresponded to the addition of activated serpentine powder through one of the lid ports using a funnel. The same port could host an adapter for a syringe that was used to remove small samples of slurry at given time intervals. Experiments were planned to be carried out at varying temperatures (T = 30, 50, 60, 90°C), partial pressures of CO_2 (p_{CO2} = 0.1 and 1 bar, 150 ml min^{-1} flow rate), slurry densities (S/L = 5, 10, 15, 20 % wt.), and a stirring rate of 600 rpm. Experiments can also be performed by dosing serpentine step by step in 1 g portions at specific time intervals during the first 2 hours, and then letting the reaction proceed for another 2 h thereafter. The intervals for feed addition were distributed linearly, exponentially, and logarithmically over the two hours of dosing. At the end of the experiments, the slurry was immediately filtered and dried at 40°C under vacuum overnight. The low drying temperature was chosen to prevent transformation of the product carbonates, and vacuum prevented potential further carbonation of the moist filter cake. The mother liquor was used to synthesize pure Mg-carbonates, either by keeping it for three days at room temperature and atmospheric p_{CO2}, or by heating it up to 90°C at 0.1 bar p_{CO2}.

Another series of experiments was performed in a similar temperature and gas flow controlled crystallizer, but with a ball-mill loop attached. Using a peristaltic pump, slurry was continuously removed from the reactor, piped into the drum of a ball-mill, and back into the reactor. The pump rate was set to result in a mean residence time of the slurry in the milling drum of one minute. A disc filter prevented the grinding medium, 1.5 mm zirconia beads, from leaving the drum together with the slurry. Following the same procedure as described before, ultrapure water was equilibrated in the crystallizer, before being pumped into the drum. While filling, the entire mill was kept in upright position to avoid entrapment of air in the drum. Then, the serpentine was added into the crystallizer and turning-on of the mill denoted the start of an experiment. Experiments were planned to be carried out at 10% wt. *S/L* ratio and 1 bar p_{CO2}, applying different temperatures (30, 50, 60°C) and milling intensities (600, 800, 1200, 2400 rpm). Studying higher temperatures would not be possible due to insufficient insulation of the tubing and milling drum. Product handling followed the same procedure as described above.

3.2. Analytical

Dry product was characterized using x-ray diffraction (Bruker, AXS D8 Advance) and scanning electron microscopy (Zeiss, LEO 1530). Thermogravimetric analysis (Mettler Toledo, TGA/SDTA851) was used to determine the extent of carbonation, R_x. TGA of Mg-carbonates is very sensitive to heating rate, isothermal sections, sample amount, and the atmosphere in the furnace (see [9] for a discussion). When heated up, nesquehonite can transform into hydromagnesite even under dry conditions, given the presence of some residual water vapor [10]. Therefore, the analyses have been performed under a 50 ml min^{-1} nitrogen flow and the amount of sample (150 mg), temperature ramp (40-900°C), and heating rate (10°C min^{-1}) were kept constant for all measurements. Knowing the carbonate content, x_{CO2}, of the product, and the Mg content of the solid feed, $x_{Mg,0}$, the extent of carbonation, R_x, of each sample was calculated according to:

$$R_x = \frac{x_{CO_2}}{1-x_{CO_2}} \frac{M_{Mg}}{x_{Mg,0} M_{CO_2}}, \tag{1}$$

where M_{Mg} and M_{CO2} are the molar masses of magnesium and CO_2, respectively.

4. Results and discussion

4.1. TGA analysis of Mg-carbonates

In order to understand, how the TGA measurements were to be interpreted, the pure Mg-carbonates were analyzed first. XRD analysis revealed the precipitate from the solution kept at room conditions to be nesquehonite, and from the solution brought to high temperature 0.1 bar p_{CO2} to be hydromagnesite. Fig. 2 shows their corresponding thermogravimetric (TG), differential thermogravimetric (DTG, the first derivative of the TG curve), and differential thermal (DT, the difference between the sample temperature and a reference, normally an empty crucible) curve.

With 70.3% and 56.1%, the total mass loss was in excellent agreement with the theoretical value of 70.9% and 56.9% for nesquehonite and hydromagnesite, respectively. Nesquehonite lost its crystal water endothermically between 100°C and 300°C. Decarbonation started at 380°C and a remarkable sudden mass loss occurred at 500°C. This step was exothermic, as seen by the upward spike in the DT curve.

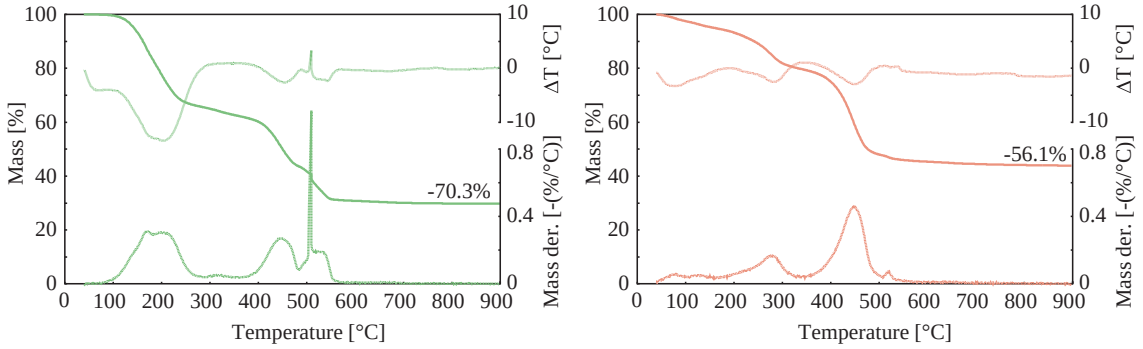

Fig. 2. TG- (solid), DTG- (dashed), and DT-curves (dotted) of nesquehonite (left, green) and hydromagnesite (right, red).

Such behavior has been reported, both for nesquehonite and hydromagnesite, at the same heating rate, but unlike here in 1 bar p_{CO2} atmosphere [11]. It has been explained by the recrystallization of magnesite via gas solid reaction. Hollingbery et al. [9] showed this exotherm to be larger the faster the heating rate. Within the cylindrical crucible, the CO_2 pressure can locally become close to 1 bar during fast decarbonation, which explains why it was observed here despite the nitrogen atmosphere. Sawada et al. [11] reported the recrystallized magnesite to decompose not before 630°C. However, according to our data, the second decarbonation step seemed to take place right after the exotherm up to approximately 550°C. Hydromagnesite lost adsorbed water already below 100°C. This follows from the platelet like morphology of hydromagnesite crystals, which provides a lot of surface for water vapor to adsorb. Between 200°C and 350°C, the basic hydroxyl groups were removed, followed by decarbonation. Interestingly, the sharp exotherm seems to be absent in our data.

Based on these findings, the carbonate content, x_{CO2}, needed to calculate R_x according to Eq. 1, was calculated consistently for all experiments. It was defined to be the weight loss between 380°C and 550°C based on the weight at 380°C, where all adsorbed and crystal water as well as the hydroxyl groups will be removed already:

$$x_{CO_2} = \frac{\Delta m_{380-550°C}}{m_{380°C}}. \quad (2)$$

4.2. Single-step carbonation experiments with and without concurrent grinding

Monitoring the reacting slurries with Raman proved to be efficient to follow the evolution of products, despite the strong background in the spectra, which was caused by the presence of the pseudo amorphous serpentine feed. Fig. 3 shows Raman spectra of three preliminary experiments at 30, 60, and 90°C, together with SEM images of the acquired product. At 30°C, the needle shaped crystals of nesquehonite remained prevalent over the entire experimental runtime. At 60°C, the transformation of nesquehonite into hydromagnesite ($Mg_5(CO_3)_4(OH)_2.4H_2O$) could be confirmed and the product was dominated by platelet shaped hydromagnesite. At 90°C, hydromagnesite formed with minimal delay after addition of the feedstock. The transformation from nesquehonite into hydromagnesite was also observed when heating the mother liquor of the 30°C experiment rapidly beyond temperatures of 50°C.

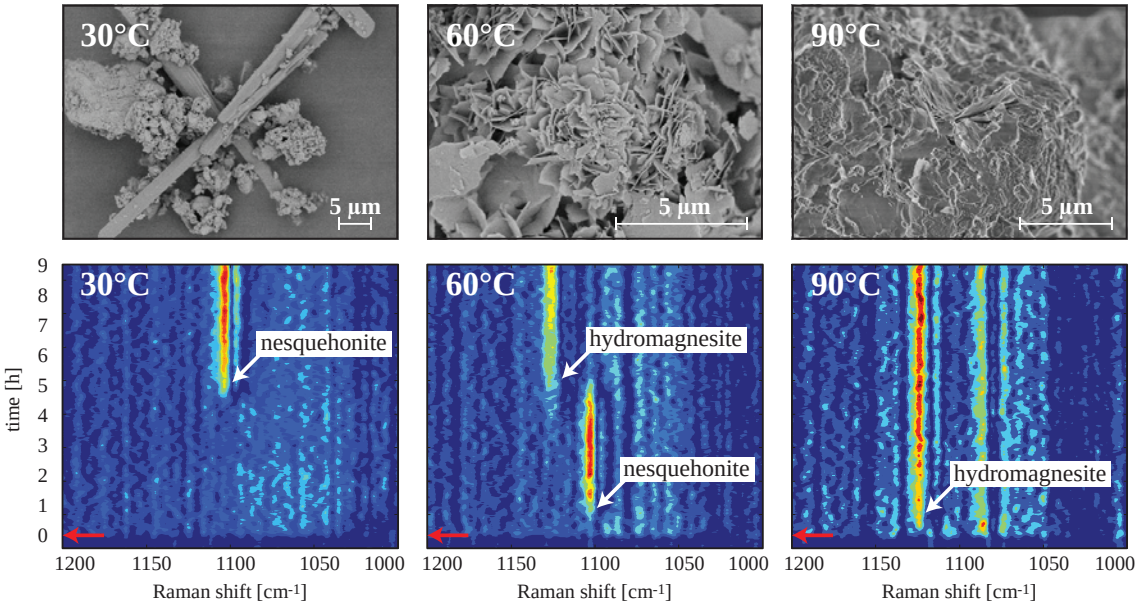

Fig. 3. SEM images (top) of product for experiments at 30°C (left), 60°C (middle), and 90°C (right). Contour plots of Raman spectra (bottom), color map relative to gradient of spectra in x-direction. Red arrows denote serpentine addition. Raman shift values for nesquehonite is 1099 cm^{-1}, and for 1119 $cm^{-}1$ for hydromagnesite. Experimental conditions: p_{CO2} = 1 bar, *S/L* = 10% wt.

However, the amount of carbonates that formed within 9 h reaction time was rather limited. In fact, only 12.6%, 16.2%, and 16.0% carbonation was measured for the experiments at 30, 60, and 90°C, respectively. Somewhat higher was the R_x for a run at 50°C (R_x = 19.9%, not shown in Fig. 3) where nesquehonite was identified in the product. Not surprisingly, lower p_{CO2} as well as a lower *S/L* ratio did not yield higher efficiencies (R_x = 6.9% at p_{CO2} = 0.1, *S/L* = 10% wt., *T* = 90°C; and R_x = 2.0% at p_{CO2} = 1bar, *S/L* = 5% wt., *T* = 30°C). Increasing the *S/L* ratio to 15 and 20% wt. reduced the time until onset of precipitation and increased the carbonation efficiency at 30°C, but the R_x did not exceed 20% for all four temperatures investigated. At these high slurry densities, the pH jumped up to levels above 9, which was suspected to be much too high for serpentine dissolution to proceed.

In an attempt to prevent such high pH, the serpentine was dosed step by step. Fig. 4 shows the measured pH profiles of these experiments. While the damping of the initial pH fluctuation was indeed effective, none of the three dosing strategies lead to higher carbonation efficiency than measured for the reference case, where all feed was added at once ($R_{x,reference}$ = 19.5%, $R_{x,linear}$ = 19.6%, $R_{x,logarithmic}$ = 18.6%, and $R_{x,exponential}$ = 16.8%). Therefore, it was hypothesized that further reaction progress could be hindered by the formation of a passivating layer around the dissolving mineral feed. This layer could either consist of an undissolved silica ash or it could form via heterogeneous nucleation and growth of carbonates on the serpentine surface.

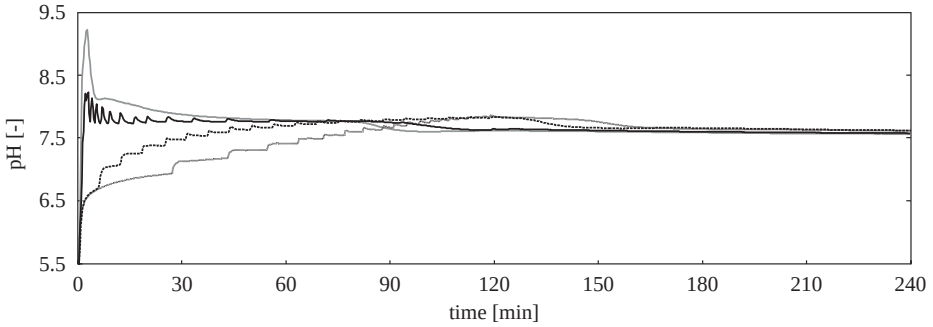

Fig. 4. pH-profiles for serpentine addition in 1 g portions at logarithmically (solid), linearly (dashed), and exponentially (dotted) distributed time intervals between 0 and 120 min. Grey solid line represents the reference case, i.e. addition of the feed at once. Experimental conditions: 30°C, p_{CO2} = 1 bar, *final S/L* = 20% wt.

Using the ball-mill set-up, this hypothesis was challenged. Concurrent grinding should effectively remove a potential passivating layer and create fresh surface for unhindered dissolution. The outcome of this experimental campaign is presented in Tab. 1 and Fig. 5, together with experiments in the EasyMax™ set-up with equal runtime (240 min), *S/L* ratio (10% wt.), p_{CO2} (1 bar) and temperature.

Table 1. Resulting extent of carbonation for experimental campaign with concurrent grinding.

Exp. No°	*T* [°C]	Milling intensity [rpm]	R_x [%]	Carbonate in product	Onset of precipitation [min]
C047-4	30	-	1.8	nesquehonite	360
M005	30	600	9.7	nesquehonite	90
M006	30	1200	12.0	nesquehonite	120
M007	30	2400	14.8	nesquehonite	20
C049-4	50	-	14.4	nesquehonite	60
M008	50	800	15.7	nesquehonite	30
M009	50	1200	17.1	nesquehonite	30
M010	50	2400	8.9	nesquehonite→hydromagnesite	30→90
C045-4	60	-	12.3	nesquehonite (→ hydromagnesite)	45 (→300)
M012	60	800	18.6	nesquehonite→hydromagnesite	30→220
M013	60	1200	24.6	nesquehonite→hydromagnesite	30→240

The ball-mill was effective in reducing the time till onset of precipitation, most significantly at 30°C. Apparently, the concurrent grinding did promote serpentine dissolution until the solutions got supersaturated with respect to the Mg-carbonates. Also, the time and temperature needed for the onset of nesquehonite to hydromagnesite transformation was reduced. However, from Fig. 5 it can be observed that only at the lowest temperature investigated the R_x could be considerably increased relative to the reference run without concurrent grinding. To recall, this trend was also observed when increasing the *S/L* ratio from 10% to 20% wt. at 30°C and 1 bar p_{CO2}. At 50°C and 60°C, the increase in R_x with the milling intensity was only marginal. In fact, at 50°C, the highest intensity yielded a deleterious effect, which could be explained by the re-dissolution of precipitates upon excessive comminution. It has to be noted, however, that experimental difficulties put this result in question. At high stirring rates and temperature,

the lower viscosity of the slurry caused heavier particles to accumulate in the tubing, so that a substantial part of the feed was excluded from the grinding loop.

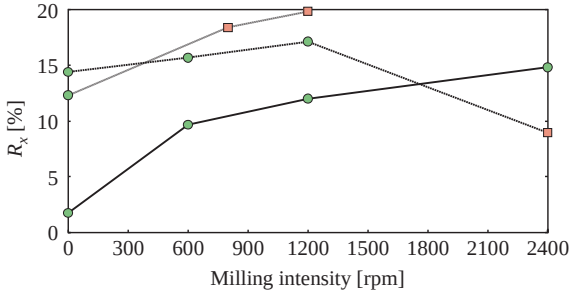

Fig. 5. Milling intensity vs. R_x for 30°C (solid), 50°C (dashed), and 60°C (dotted). Green circles represent experiments with nesquehonite in the product, red squares those where the transformation from nesquehonite to hydromagnesite (or the onset thereof) was observed. Experimental conditions: p_{CO2} = 1 bar, *S/L* = 10% wt.

Generally, the ineffectiveness of concurrent grinding suggested equilibrium effects to be the actual reason for the low values of R_x in our single-step experiments. Both the activated serpentine and the Mg-carbonates are more soluble in an acidic environment, leading to a trade-off regarding the pH-level in single step carbonation. The higher the alkalinity of the solution (i.e. the more Mg^{++} dissolved), the lower the solubility of the carbonates, but the fewer protons are available for serpentine dissolution. As demonstrated in Fig. 4, the pH increased very rapidly upon adding all solids at once. Thereafter, solution absorbed more CO_2, which reduced the pH and enabled magnesium leaching to continue slowly, until supersaturation was high enough for nucleation and growth of carbonates to occur. The more or less sudden consumption of magnesium is reflected in a small pH-drop short before 90 min for the reference case. Thereafter, the solution could be at or close to equilibrium, such that further reaction progress was either very slow or impossible at all. Remarkably, in all experiments where the pH was monitored, it stabilized around pH = 7.5, depending primarily on the runtime and p_{CO2} (see Fig. 4).

5. Conclusions

This paper reports results of a research program where we study the carbonation potential of heat treated serpentine. We have carried out experiments at different operating conditions relevant for flue gas mineralization. In its simplest process form, the single-step mode, the experimentally measured extent of carbonation was found to be limited to 20% under the conditions explored in this work. We have tried to enhance the performance of the process by damping the initial sharp increase of pH by dosing the feed in a stepwise mode, or by creating a fresh reactive serpentine surface by concurrent grinding. These experiments have exhibited promising results, which are however not yet conclusive. The key challenge of the single-step process is the fact that dissolution of serpentine and precipitation of magnesite are favored at the opposite ends of the pH range. Upon onset of precipitation, the equilibrium pH in the system activated-serpentine-CO_2-H_2O is too high for further dissolution, but too low for further precipitation. We are now actively exploring the operating conditions of the one-step process in order to find the best trade-off among these conflicting needs. Further we believe that the overall carbonation efficiency may improve, if serpentine dissolution and Mg-carbonate precipitation are separated. This can be achieved at the price of enhanced process complexity, but with better control of critical operating conditions. Currently, such double-step experiments are being carried out. A temperature swing in combination with a p_{CO2} swing shows promising results and indicates substantial room for optimization.

Nomenclature

m	mass [mg]
M	molar mass [g mol^{-1}]
p_{CO2}	partial pressure of CO_2 in the reactor [bar]
R_x	extent of carbonation [%]
S/L	solid liquid ratio of the slurry (synonym: slurry density) [%]
T	Temperature [°C]
x_{CO2}	carbonate content in product [%]
$x_{Mg,0}$	magnesium content of solid feed [%]

Acknowledgements

We would like to thank Dr. Marcel Verduyn and Gert van Mossel from Shell GSI, Amsterdam, the Netherlands, for providing the activated serpentine used in this study.

References

[1] Verduyn MA, Boerringter H, Oudwater R, van Mossel GAF. A novel process concept for CO_2 mineralization; Technical opportunities and challenges. In: *5th Trondheim Conference on CO2 Capture, Transport and Storage*, Trondheim, Norway; 2009.

[2] McKelvy MJ, Chizmenshya AVG, Diefenbacher J, Bearat H, Wolf G. Exploration of the role of heat activation in enhancing serpentine carbon sequestration reactions. *Environ Sci Technol* 2004;**38**:6897–903.

[3] O'Connor WK, Dahlin DC, Rush GE, Gerdemann SJ, Penner LR, Nilsen DN. Aqueous mineral carbonation: mineral availability, pretreatment, reaction parametrics and process studies. DOE/ARC-TR-04-002, Albany Research Center; 2005.

[4] Kittrick JA, Peryea FJ. Determination of the Gibbs free energy of formation of magnesite by solubility methods. *Soil Sci Soc Am J* 1986;**50**:243–7.

[5] Hänchen M, Prigiobbe V, Baciocchi R, Mazzotti M. Precipitation in the Mg-carbonate system – effects of temperature and CO_2 pressure. *Chem Eng Sci* 2008;**63**:1012–28.

[6] Wolery TJ. EQ3/6, a software package for geochemical modeling of aqueous systems: package overview and installation guide (version 7.0). UCRL-MA-110662 PT I, Lawrence Livermore National Laboratory; 1992.

[7] Zhang Z, Zheng Y, Ni Y, Liu Z, Chen J, Liang X. Temperature- and pH-dependent morphology and FT-IR analysis of magnesium carbonate hydrates. *J Phys Chem* 2006;**110**:12969–73.

[8] Davies PJ, Bubela B. The transformation of nesquehonite into hydromagnesite. *Chem Geol* 1973;**12**:289–300.

[9] Hollingbery LA, Hull TR. The thermal decomposition of huntite and hydromagnesite. *Thermochim Acta* 2010;**509**:1–11.

[10] Dell RM, Weller SW. The thermal decompostion of nesquehonite $MgCO_3.3H_2O$ and magnesium ammonium carbonate $MgCO_3.(NH_4)_2CO_3.4H_2O$. *T Faraday Soc* 1959;**55**:2203–20.

[11] Sawada Y, Yamaguchi J, Sakurai O, Uematsu K, Mizutani N, Kato M. Thermal decomposition of basic magnesium carbonates under high-pressure gas atmoshpheres. *Thermochim Acta* 1979;**32**:277–291.